Turbulent Dissipation Rates, Mixing, and Heat Fluxes in the Canadian Arctic from Glider-based Microstructure Measurements

Benjamin Scheifele[1], Stephanie Waterman[1] and Jeff Carpenter[2]

[1]Department of Earth, Ocean and Atmospheric Sciences, University of British Columbia, Vancouver, Canada
[2]Institute of Coastal Research, Helmholtz-Zentrum Geesthacht, Geesthacht, Germany

contact B. Scheifele at bscheife@eos.ubc.ca

Abstract

We present new observations from a microstructure-equipped ocean glider in the southeastern Beaufort Sea of the Canadian Arctic. The glider measured 345 quasi-vertical profiles of microstructure shear and finescale temperature and salinity. We use these measurements to calculate the rate of dissipation of turbulent kinetic energy and to assess the strength of turbulent mixing. The region is characterized by strong stratification, and we find that despite dissipation rates varying across four orders of magnitude, turbulence is only rarely energetic enough to create a meaningful buoyancy flux. In the vast majority of our measurements, turbulent mixing is inhibited by the stratification.

1 Introduction

This article presents our study of mixing in the southeastern Beaufort Sea of the Arctic Ocean; it's ultimate goal is to understand mixing rates and associated heat fluxes in the Canada Basin thermocline. To do this, we measure ocean turbulence because, in the absence of vertical advective motion, mixing due to turbulence is thought to be the primary mechanism by which heat is transported vertically in the watercolumn. The vertical transport of heat remains a key topic in studies of the Arctic Ocean because oceanic heat fluxes are a prime candidate for explaining enhanced heat fluxes to the floating sea ice pack which has been melting at unprecedented rates over the last three decades.

Warm water containing enough heat to melt the entire Arctic Ocean sea-ice pack in the span of a few years circulates horizontally in the Canada Basin between 200-800 m depth (Turner, 2010). This water, the largest integrated source of heat to the Arctic Ocean, is associated with inflow from the Atlantic Ocean and has a temperature maximum at 400 m depth. It is trapped below a $\sim$100 m thick layer of colder (but fresher) water of Pacific origin, effectively isolating it from the surface mixed layer and the overlying sea ice.

Despite a number of studies which have used various methods to quantify the flux of heat from the warm Atlantic Water layer upwards through the thermocline, our understanding of the size and distribution of vertical heat fluxes remains in many ways a mystery (Carmack et al., 2015). In the study described below, we measured temperature, salinity, and microstructure shear in one geographic region of the Beaufort Sea. From these measurements, we calculate turbulent dissipation and mixing rates in order to estimate heat fluxes through the thermocline.

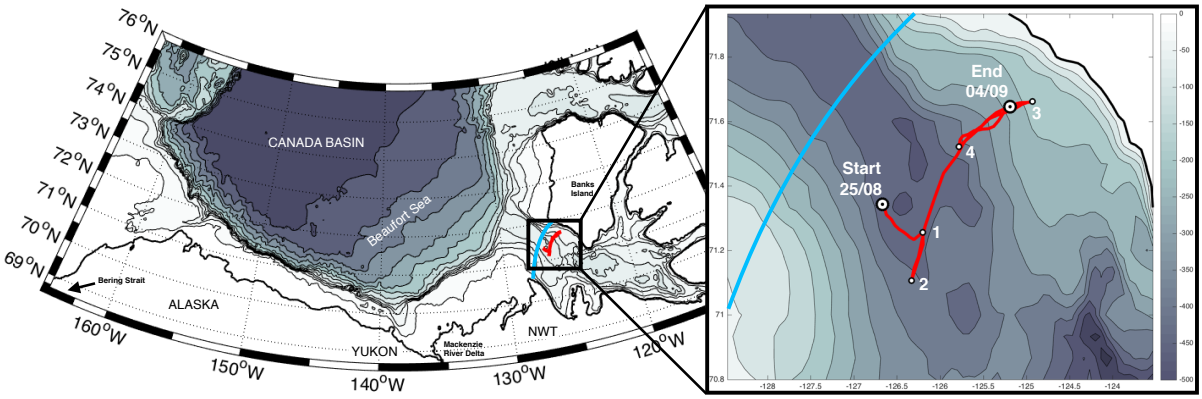

Figure 1: The glider's 10 day path in the Amundsen Gulf along which it measured 345 quasi-vertical CTD and microstructure profiles in summer 2015. Shown are the start and end points/dates, as well as the location of four intermediate waypoints. The light-blue line indicates approximately the north-eastern boundary beyond which it was unsafe to operate the glider because of the possibility of sea ice or sea ice melt.

2 Methods and Background

2.1 Overview

We used an autonomous ocean glider to measure 345 quasi-vertical profiles of microstructure velocity shear and finescale conductivity, temperature, and depth (CTD) in the Amundsen Gulf of the southeastern Beaufort Sea. The glider profiled continuously over the 10-day period 25 Aug — 04 Sept 2015 along the track depicted in Figure 1. It began its mission in the central Amundsen Gulf, briefly headed south before turning about, and then traversed the continental shelf slope on the northern side of the Gulf three times. During the first 45 kms (3 days), the glider dove to a fixed depth of 300 m; afterwards it began bottom-tracking and dove to within 15 m of the bottom.

From the shear measurements, we compute profiles of the rate ϵ of dissipation of turbulent kinetic energy. We use these in conjunction with the CTD measurements to characterize the variability of turbulence and the strength of turbulent mixing in our study region. The glider and microstructure instrument are described in Section 2.2, the processing of the microstructure data in Section 2.3, and methods for assessing mixing strength in Section 2.4. Results are presented in Section 3.

2.2 Glider and MicroRider

The platform for our CTD and microstructure measurements was a 1000 m capable Slocum G2 ocean glider, equipped with a microstructure package manufactured by Rockland Scientific. An ocean glider is a high-endurance autonomous underwater vehicle which propels itself through the water by adjusting its buoyancy to create vertical motion. This in turn is translated into horizontal motion by a pair of fixed wings, creating a zig-zag motion through the water column as the instrument rises and sinks. It adjusts its heading with a small electronic tail fin and glides at a nominal velocity of 0.3 m/s at an angle of about 25° to the horizontal.

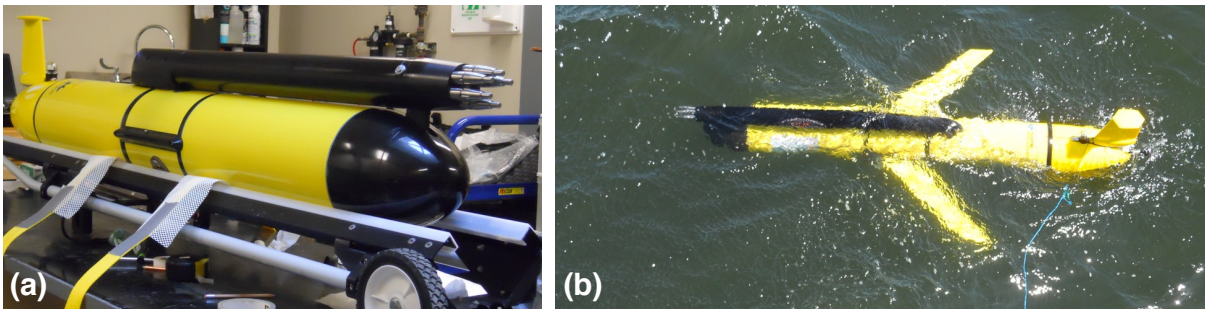

Figure 2: The glider used as the platform for our measurements (a) on the lab bench with the wings removed, and (b) during deployment, shown here with a temporary safety-tether. The microstructure probes are mounted above and to the front of the instrument, and the end of the black cylindrical housing. The CTD, mounted on the port side below the wing, is not visible in these views.

When on a mission, the glider attempts to follow a predefined series of waypoints, navigating with its internal compass and accelerometers. It surfaces at predetermined intervals to obtain a GPS-fix and communicate via satellite with the pilot to receive updated flight-instructions and waypoints. The on-board CTD manufactured by SeaBird is pumped and, in our case, programmed to run continuously. The externally mounted microstructure package contains two orthogonally oriented aerofoil velocity shear probes which sample at 512 Hz. It additionally houses two microstructure temperature probes, whose data we do not discuss further here; these will be the topic of a future study.

It is worth mentioning that microstructure measurements from an ocean glider are novel: the first study to use a microstructure equipped glider in a realistic setting is that by Fer et al. (2014). Nonetheless, gliders have proven to be excellent platforms for sensitive ocean microstructure measurements because, in stark contrast to a surface ship, they contain few moving parts and produce little mechanical vibration. As a result, the resolution of turbulence measurements from gliders is comparable to that of the best free-falling microstructure instruments, with the added advantage that individual profiles do not require manual labour and supervision.

2.3 Microstructure Processing

Each shear probe signal provides centimetre-scale velocity shear $\partial u/\partial z$, where u is velocity in the direction of the probe orientation (perpendicular to the motion of the glider) and z is the spatial coordinate along the glider's path. Assuming isotropic turbulence, the dissipation rate ϵ can be calculated by integrating spectra of the measured velocity-shear variance over the wavenumbers k at which turbulent dissipation occurs:

$$\epsilon = (15\,\nu/2)\left\langle(\partial u/\partial z)^2\right\rangle = (15\,\nu/2)\int_{\mathrm{k_{min}}}^{\mathrm{k_{max}}}\Phi(k)\,\mathrm{d}k \quad , \tag{1}$$

where ν is the kinematic viscosity and $\Phi(k)$ is the calculated spectrum of velocity-shear variance per unit wavenumber. For each ϵ estimate, we calculate spectra from ten consecutive half-overlapping 4-second windows, average the ten spectra, and then integrate. The integration limits $\mathrm{k_{min}}$ and $\mathrm{k_{max}}$ are chosen to maximize the integration range while excluding measurement noise at excessively large wavenumber (Figure 3). We integrate from the lowest resolved wavenumber (typically O(1) cpm) to the onset of noise in the

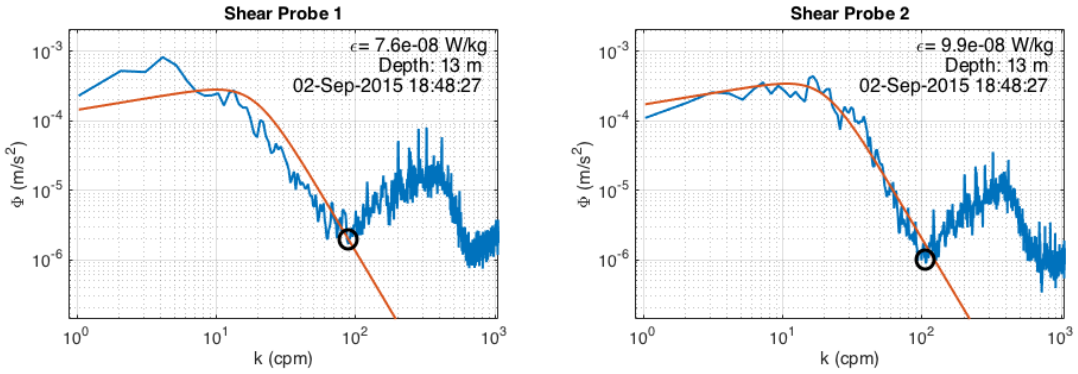

Figure 3: Two selected simultaneous velocity-shear spectra (blue). We integrate from the lowest available wavenumber to the upper integration limit k_{max} (black circles) where the noise begins to dominate. For reference only, a fitted Nasmyth curve (red) is shown with each spectrum.

measurements (typically O(10) cpm). We explicitly integrate the *measured* spectrum rather than a "universal" curve such as the Nasmyth spectrum.

2.4 Estimating Mixing

Mixing in the ocean can be characterized by the diffusivity of density K_ρ which, at steady state, may be parameterized in terms of ϵ by

$$K_\rho = \Gamma \epsilon / N^2 \tag{2}$$

where $N = \sqrt{(g/\rho_o)(\mathrm{d}\rho/\mathrm{d}z)}$ is the buoyancy frequency and Γ is a dimensionless "mixing efficiency". The value $\Gamma = 0.2$ from Osborn (1980) is often adopted for this calculation, but mounting evidence from numerical and lab studies suggests that Γ is in fact variable and depends on the characteristics of the flow and the ambient stratification. For example, Ivey et al. (2008) outline how $\Gamma \to 0$ as the stratification becomes either too small or too large, in which case the diffusivities of salt and heat (and thus also density) revert to their molecular values.

The effect of stratification on turbulent mixing can be quantified through a turbulence intensity parameter

$$I = \epsilon / \nu N^2 \tag{3}$$

which characterizes the strength of turbulent stirring relative to the stabilizing effects of stratification. Lab experiments by Stillinger et al. (1983) suggest that there is no meaningful buoyancy flux (i.e. no turbulent mixing) when $I < 24.5$. Early direct numerical simulations by Itsweire et al. (1993) similarly suggest that turbulent mixing is insignificant when $I < 19$. Likewise, a numerical study by Shih et al. (2005) highlights that turbulent mixing can be described in three distinct regimes: $I < 7$ where turbulent mixing is suppressed and diffusion occurs by molecular processes, a transitional regime of intermediate mixing when $7 < I < 100$, and fully turbulent mixing which exists only when $I > 100$. From the combined results of these studies, it seems likely that there is a critical threshold at $I = \mathrm{O}(10)$ below which turbulence is too weak to overcome stratification and drive diapycnal mixing.

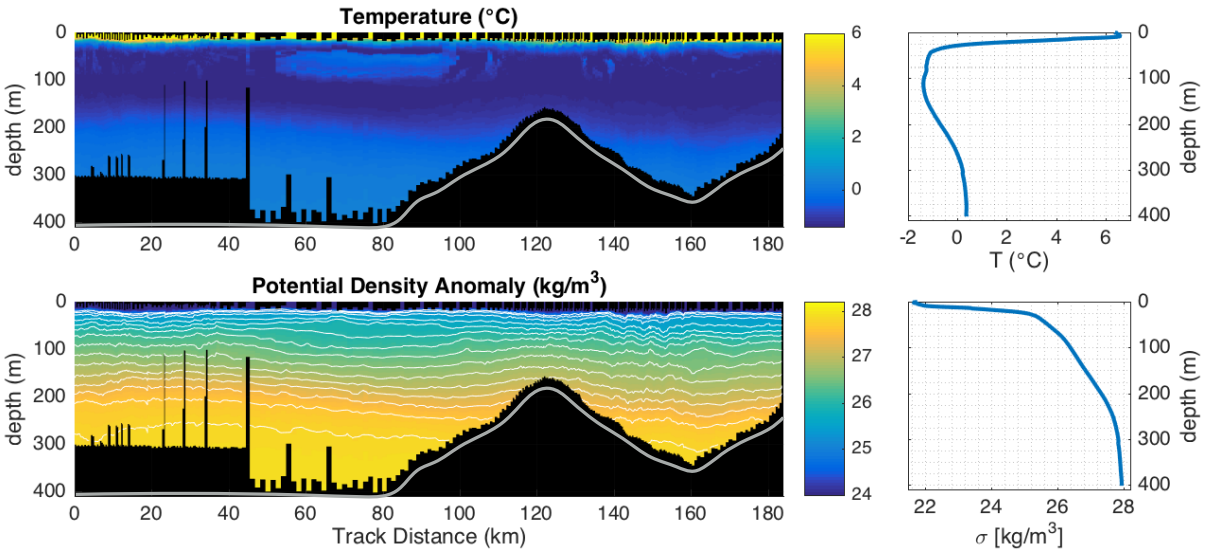

Figure 4: (**Left**) Temperature and density sections along the glider track shown in Figure 1. Isopycnals in 0.2 kg/m^3 increments are shown in white in the lower figure. The approximated bathymetry is shown in grey for reference. (**Right**) Mean temperature and density profiles.

3 Results

3.1 Large-scale characteristics

The large-scale temperature and density fields measured by the glider are shown in Figure 4. It is evident from these that the watermass structure in the Amundsen Gulf, despite being at the geographic margins of the Arctic Ocean, exhibits the same primary features that define the structure in the central Canada Basin. These include a seasonal thin, fresh and warm surface mixed layer; a remarkably strong near-surface pycnocline resulting from summer sea ice-melt; a colder temperature minimum below the surface mixed layer associated with Pacific inflow; the thermocline at the transition to warmer Atlantic-origin water, and finally the warm Atlantic Water temperature maximum at ∼350–400 m depth. In addition, the strong stratification above 300 m, the presence of a distinctive warm-core mesoscale eddy, and the clear signature of isopycnal displacement due to internal waves are all representative of features found in the central basin.

3.2 Turbulent characteristics and mixing

The dissipation rate of turbulent kinetic energy, shown in Figure 5, is generally small but also variable and patchy. The cross-section reveals that patches with ϵ values of order 10^{-9} W/kg are superimposed on a background state of order 10^{-10} W/kg. This is comparable to open ocean dissipation rates away from ridges or rough topography in the Pacific and Atlantic Oceans (Waterhouse et al., 2014). A small trend for bottom enhanced dissipation rates below 200 m depth can be seen in the cross-sectional view (Figure 5a) and in the survey-averaged vertical profile of ϵ (Figure 5b), highlighting the potential role of friction at the bottom boundary in setting the background turbulence environment. In contrast to recent observations by Rippeth et al. (2015), we observe the largest dissipation rates not on the continental shelf slope, but above the flat bottomed region of the Gulf, near

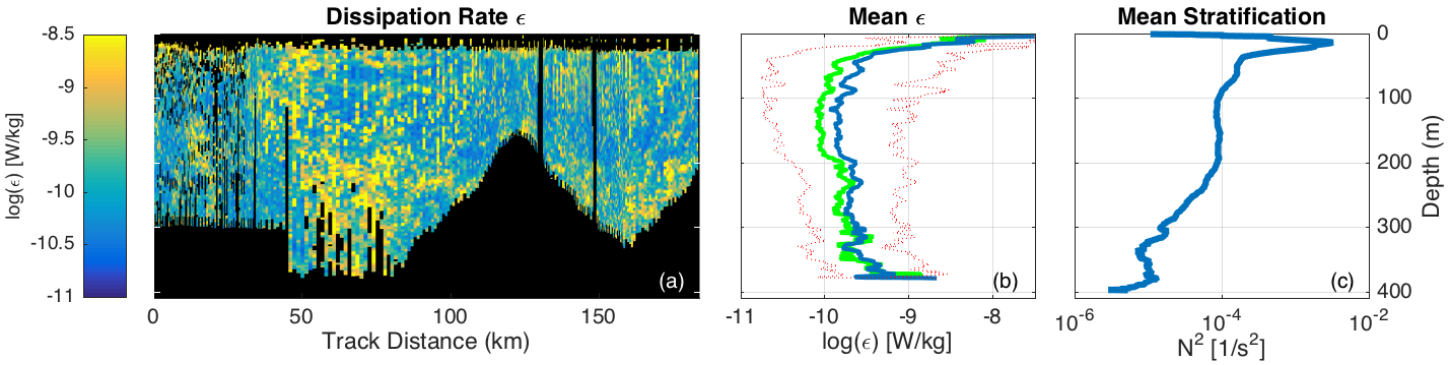

Figure 5: (**a**) A cross-sectional view of the dissipation rate of turbulent kinetic energy along the glider track. Contoured is $\log_{10}(\epsilon)$, as measured by one of the two shear probes. (**b**) The survey-averaged mean (blue) vertical profile of ϵ, plus or minus 1 standard deviation (red). The median profile (green) is also shown for comparison. (**c**) The mean stratification profile N^2 measured by the glider, needed together with ϵ to obtain mixing estimates

the boundary to the slope. The stratification, which dampens the effects of turbulence, is characterized by N^2 (Figure 5c); it is high at mid-depth, peaks below the surface mixed layer, and weakens towards the bottom boundary.

Histograms are helpful to better appreciate the turbulence measurements shown in Figure 5. In Figure 6, we present probability distributions of the dissipation rate ϵ, the ratio ϵ_1/ϵ_2 of the dissipation rate measured by the two shear probes, and the turbulence intensity parameter I. The first panel (6a) highlights three important characteristics: (i) the remarkably large variability of dissipation rates, spanning four orders of magnitude in our measurements, (ii) the disproportionately high probability of observing low dissipation rates, and (iii) the sufficiency of our measurements to successfully create statistical averages, a rarity for ocean microstructure measurements, especially in the Arctic Ocean. The interquartile range (central 75%) of the $N = 48,857$ unique dissipation rate estimates is $6{\times}10^{-11}$ — $4{\times}10^{-10}$ W/kg.

The second panel (6b) highlights that the vast majority (90%) of our $n = 17,761$ duplicate measurements agree within a factor of five. The term "duplicate" is used here to describe two ϵ estimates derived from simultaneously measured shear-variance by the two separate shear probes.

The third panel (6c) is perhaps the most striking of the three. It demonstrates that an overwhelming majority (89%) of measurements occur at $I \leq 10$. As outlined in Section 2.4, this indicates that turbulence is not energetic enough to drive a meaningful buoyancy flux in light of the stabilizing effect of the stratification, suggesting that the standard parameterization for turbulent mixing given by Equation 2 is not applicable here. Instead, we estimate that the diffusion coefficient for heat is most frequently near its molecular value $K_T \sim 10^{-7}$ m^2/s and is only occasionally enhanced by turbulent mixing. Such a low diffusion coefficient has important implications for mixing and would imply a heat flux of only 0.01 W/m^2 through the steepest part of the thermocline. While low, this value is roughly comparable to previous estimates from the central Canada Basin (Carmack et al., 2015).

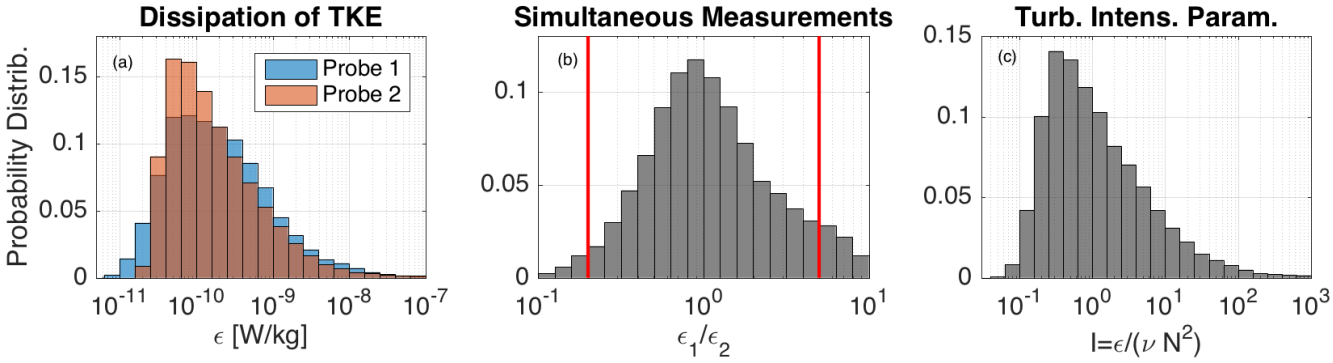

Figure 6: Probability distributions of (**a**) Dissipation rate of turbulent kinetic energy from the two shear probes; (**b**) Ratio of simultaneous ϵ measurements from the two shear probes. The region between the red lines indicates where measurements from the two probes agree to within a factor of five; (**c**) Turbulence intensity parameter, as defined by Equation 3.

4 Summary and Conclusions

In this study, we find that turbulent energetics are too weak to drive meaningful turbulent mixing in the southeastern Beaufort Sea. The natural variability of the dissipation rate of turbulent kinetic energy is high, varying by more than four orders of magnitude, but the stratification is exceptionally strong through the thermocline, and this inhibits mixing. The turbulence intensity parameter I suggests that the background turbulent state would have to increase by at least an order of magnitude to drive a meaningful buoyancy flux. The study of mixing in the Arctic Ocean has become popular because the warm Atlantic Water layer which is trapped below the pycnocline contains substantial heat, but it is not clear exactly where and how quickly this heat mixes through the thermocline. Our study of mixing in the Amundsen Gulf at the margin of the Beaufort Sea suggests that vertical fluxes of heat due to turbulent mixing are small and largely inconsequential when the stratification is as high as it was in our measurements.

Acknowledgements

We thank Lucas Merckelbach of HZG and the Ocean Tracking Network Group at Dalhousie University for their invaluable help with the glider preparations. We also thank ArcticNet Canada and the crew of the CCGS Amundsen who assisted with this work. The Canadian partners were supported by the Canadian Arctic GEOTRACES Program, a Vanier Canada Graduate Scholarship, a UBC Killam Doctoral Scholarship, the UBC Four Year Fellowship Program, and the Northern Scientific Training Program.

References

Carmack, E., Polyakov, I., Padman, L., Fer, I., Hunke, E., Hutchings, J., Jackson, J., Kelley, D., Kwok, R., Layton, C., Melling, H., Perovich, D., Persson, O., Ruddick, B., Timmermans, M. L., Toole, J., Ross, T., Vavrus, S., and Winsor, P. (2015). Toward Quantifying the Increasing Role of Oceanic Heat in Sea Ice Loss in the New Arctic. *Bulletin of the American Meteorological Society*, 96(12):2079–2105.

Fer, I., Peterson, A. K., and Ullgren, J. E. (2014). Microstructure Measurements from an Underwater Glider in the Turbulent Faroe Bank Channel Overflow. *Journal of Atmospheric and Oceanic Technology*, 31(5):1128–1150.

Itsweire, E. C., Koseff, J. R., Briggs, D. A., and Ferziger, J. H. (1993). Turbulence in Stratified Shear Flows: Implications for Interpreting Shear-induced Mixing in the Ocean. *Journal of Physical Oceanography*, 23:1508–1522.

Ivey, G. N., Winters, K. B., and Koseff, J. R. (2008). Density Stratification, Turbulence, but How Much Mixing? *Annual Review of Fluid Mechanics*, 40(1):169–184.

Osborn, T. R. (1980). Estimates of the Local Rate of Vertical Diffusion from Dissipation Measurements. *Journal of Physical Oceanography*, 10(1):83–89.

Rippeth, T. P., Lincoln, B. J., Lenn, Y.-D., Green, J. A. M., Sundfjord, A., and Bacon, S. (2015). Tide-mediated warming of Arctic halocline by Atlantic heat fluxes over rough topography. *Nature Geoscience*, 8(3):191–194.

Shih, L. H., Koseff, J. R., Ivey, G. N., and Ferziger, J. H. (2005). Parameterization of turbulent fluxes and scales using homogeneous sheared stably stratified turbulence simulations. *Journal of Fluid Mechanics*, 525:193–214.

Stillinger, D. C., Helland, K. N., and Van Atta, C. W. (1983). Experiments on the transition of homogeneous turbulence to internal waves in a stratified fluid. *Journal of Fluid Mechanics*, 131:91–122.

Turner, J. S. (2010). The Melting of Ice in the Arctic Ocean: The Influence of Double-Diffusive Transport of Heat from Below. *Deep Sea Research*, 40(1):249–256.

Waterhouse, A. F., MacKinnon, J. A., Nash, J. D., Alford, M. H., Kunze, E., Simmons, H. L., Polzin, K. L., Laurent, L. C. S., Sun, O. M., Pinkel, R., Talley, L. D., Whalen, C. B., Huussen, T. N., Carter, G. S., Fer, I., Waterman, S. N., Garabato, A. C. N., Sanford, T. B., and Lee, C. M. (2014). Global Patterns of Diapycnal Mixing from Measurements of the Turbulent Dissipation Rate. *Journal of Physical Oceanography*, 44(7):1854–1872.